Nuclear Physics **A528** (1991) 436–446
North-Holland

HEAVY-ION EXCITATION OF GIANT RESONANCES AT INTERMEDIATE ENERGIES

A.N.F. ALEIXO and C.A. BERTULANI

Instituto de Física, Universidade Federal do Rio de Janeiro, Cidade Universitária-Cx. Postal 68528, 21945 Rio de Janeiro, RJ, Brazil

Received 8 November 1990
(Revised 10 December 1990)

Abstract: We develop a Glauber-type formalism to study the excitation of giant resonances in heavy-ion collisions at intermediate energies. Contributions from the nuclear and the Coulomb interaction as well as their interference are easily accomplished within this approach. Application is done for the excitation of isovector giant dipole and isoscalar giant quadrupole resonances in ^{208}Pb by means of ^{17}O projectiles at 84 MeV/nucleon laboratory energy. A good agreement with the experimental data is found. The formalism is parameter-free, having as inputs the free nucleon–nucleon cross sections, the ground-state densities and the transition densities of the nuclei.

1. Introduction

The Coulomb excitation of giant resonances in heavy-ion collisions at high energies opens new possibilities for the study of multipolarity content, relative strength, decay branching-ratios, and other aspects of giant resonances in nuclei. As compared to electron scattering there is the advantage of the coherent action of the field of the Z protons in the projectile. This increases the cross section up to a factor 10^4 for very heavy ions, as compared to electron scattering. Increasing the beam energy also increases the Coulomb excitation cross section since the ratio between the interaction time and the nuclear transition time is of order unity (or less) even for large impact parameters, $b \gg R_1 + R_2$. A drawback is that the process is accompanied by contributions from the nuclear interaction.

The experimental investigation of the excitation of giant resonances with intermediate energy heavy ions is only at its beginning. The analysis of the data of ^{17}O (84 MeV/nucleon) + ^{208}Pb performed at GANIL [1]) has shown the usefulness of the method and encourages further measurements. In that experiment the excitation of giant resonant states in ^{208}Pb was identified by a measurement of the energy loss and the scattering angle of ^{17}O is the collision. The energy transfer in the reaction is restricted to small values ($\hbar\omega \leqslant 20$ MeV) and the scattering angles are very small ($\theta \leqslant 5°$), in order to avoid the projectile or target direct breakup. These inelastic data can be explained within a DWBA prescription with optical model parameters used to fit the elastic scattering data [1]).

In this article we show that the excitation of giant resonances in intermediate-energy collisions (~100 MeV/nucleon), as in the experiment cited above, can be well described in a Glauber model [2]. There is practically no adjustable parameters needed, except for the deformation parameters β_L which characterizes the strength of the collective excitation. Amazingly, the agreement with the experimental data is very good. Due to its simplicity, this approach allows a clearer understanding of the reaction mechanism than the more time consuming DWBA recipe. Similar approaches have been successfully applied by several authors [3,4] to the study of heavy ion excitation in intermediate-energy collisions.

In the semiclassical theory of Coulomb excitation at low energies [5] the inelastic cross section can be expressed as

$$\left(\frac{d\sigma}{d\Omega}\right)_{fi} = \left(\frac{d\sigma}{d\Omega}\right)_{Rut} P_{fi}^{(1)} = \left(\frac{d\sigma}{d\Omega}\right)_{Rut} |\chi_{fi}|^2 F(\theta, \xi)\,, \tag{1.1}$$

where $P_{fi}^{(1)}$ is the probability amplitude for exciting a nuclear state f, from an initial prescribed state i, in first-order perturbation theory; $(d\sigma/d\Omega)_{Rut}$ is the Rutherford cross section; $\xi = \omega a/v$ is the adiabaticity parameter, where $a = Z_1 Z_2 e^2/2\mu v^2$ is half the distance of closest approach in a head-on collision. The strength function $|\chi_{fi}|^2$ expresses the response of the nucleus to the energy transfer $\hbar\omega$ in the collision, and $F(\theta, \xi)$ is a kinematical function depending on the scattering angle [5]. For Coulomb excitation of ^{208}Pb in the collision ^{17}O+^{208}Pb at 84 MeV/nucleon, one can show that the maximum values attained by these functions are $|\chi_{fi}|^2 \sim 0.9$ and $F(\theta, \xi) \sim 10^{-3}$, if we consider the excitation of a nuclear state with $\hbar\omega \sim 10$ MeV. This ensures the validity of first order perturbation theory for the semiclassical calculation [6]. Based on these values, the semiclassical formalism was used by some authors [e.g. ref. [6]] to study Coulomb excitation in intermediate-energy collisions with heavy ions.

The above argument is based on Coulomb excitation alone. But, for large scattering angles inelastic processes must have participation from the nuclear interaction. In this case, Coulomb–nuclear interference should also be important. Moreover, if the Coulomb excitation calculated semiclassically decreases strongly with decreasing angle, the cross sections at small scattering angles should be dominated by diffraction patterns, characteristic of strong absorption. As we show in the next sections this is indeed the situation for ^{17}O+^{208}Pb at 84 MeV/nucleon. Therefore, a theoretical analysis of the excitation of giant resonances in intermediate-energy collisions can be successfully achieved only with inclusion of the effects of the strong interaction. Exception occurs if the ions involved are very heavy ($Z_1, Z_2 \geq 50$), or if the beam energy is very large (E_{lab}/nucleon ≥ 1 GeV). In such situations the semiclassical calculations of Coulomb excitation alone give reasonable descriptions of the inelastic reactions (due to the Lorentz-contraction effect [6]).

Even when the strong interaction plays a dominant role, the reaction occurs in such a way that the nuclei keep their identities and the energy transfer to the target is small in a single collision. Therefore, the process is gentle and can be described

as a first-order perturbation. Moreover, the scattering angle is very small and this enables the use of eikonal wavefunctions for the distorted waves [2]). We follow this procedure in sect. 2 where the inelastic scattering inputs are calculated using the Tassie model [7]) for the transition density of the target. In sect. 3 we present the result of numerical calculations and discussion. Our conclusions are given in sect. 4.

2. Inelastic amplitude

In the distorted-wave-impulse approximation the amplitude for the transition of nucleus 2 from the ground state $|0\rangle$ to the excited state $|\lambda\mu\rangle$ is given by

$$f^{\lambda\mu}(\theta)=\frac{ik}{2\pi\hbar v}\int \Psi_k^*(\boldsymbol{r})\langle \boldsymbol{r},\lambda\mu|U_{\rm int}(\boldsymbol{r})|\boldsymbol{r},0\rangle\Psi_k(\boldsymbol{r})\,\mathrm{d}^3r, \tag{2.1}$$

where $\boldsymbol{k}(\boldsymbol{k}')$ is the initial (final) momentum of the projectile (nucleus 1) and $U_{\rm int}(\boldsymbol{r})$ is the interaction potential.

Using eikonal wavefunctions for the distorted waves, we obtain

$$f^{\lambda\mu}(\theta)=f_{\rm N}^{\lambda\mu}(\theta)+f_{\rm C}^{\lambda\mu}(\theta), \tag{2.2a}$$

where

$$f_{\rm N,C}^{\lambda\mu}(\theta)=\frac{ik}{2\pi\hbar v}\int \mathrm{e}^{i\boldsymbol{q}\cdot\boldsymbol{r}+i\chi(b)}\,\langle \boldsymbol{r},\lambda\mu|U_{\rm N,C}(\boldsymbol{r})|\boldsymbol{r},0\rangle\,\mathrm{d}^3r, \tag{2.2b}$$

$$\chi(b)=-\frac{k}{E}\int_{-\infty}^{\infty}\{U_{\rm C}[\sqrt{b^2+z^2}]+U_{\rm N}[\sqrt{b^2+z^2}]\}\,\mathrm{d}z$$

$$=\chi_{\rm C}(b)+\chi_{\rm N}(b), \tag{2.3}$$

and $\chi_{\rm N}(\chi_{\rm C})$ represents the phase induced by the nuclear (Coulomb) interaction $U_{\rm N}(U_{\rm C})$. For the nuclear interaction we use the $t\rho\rho$ formalism [8]), which relates the nucleon–nucleon potential to the nucleon–nucleus cross section by means of a double-folding

$$U_{\rm N}(\boldsymbol{r})=\int \mathcal{U}_{\rm N}(\boldsymbol{r},\boldsymbol{r}')\,\mathrm{d}^3r'=\langle t_{\rm NN}\rangle\int \rho_1(\boldsymbol{r}-\boldsymbol{r}')\,\rho_2(\boldsymbol{r}')\,\mathrm{d}^3r', \tag{2.4}$$

where $\boldsymbol{r}'$ is the intrinsic coordinate of the target nucleus.

The free nucleon–nucleon t-matrix $t_{\rm NN}(E)$ can be deduced from experiment. At intermediate and high energies, it can be written as

$$t_{\rm NN}(E)=-\tfrac{1}{2}i\hbar v\sigma_{\rm NN}(E)[1-i\alpha_{\rm NN}(E)], \tag{2.5}$$

where $\sigma_{\rm NN}(E)$ and $\alpha_{\rm NN}(E)$ are the total nucleon–nucleon cross section and the ratio of real to imaginary part of the forward nucleon–nucleon scattering amplitude.

We average $\sigma_{NN}(E)$ and $\alpha_{NN}(E)$ over isospin in the form

$$\langle\sigma_{NN}(E)\rangle=\frac{1}{A_1A_2}\{(Z_1Z_2+N_1N_2)\sigma_{pp}(E)+(Z_1N_2+Z_2N_1)\sigma_{pn}(E)\}. \quad (2.6a)$$

$$\langle\alpha_{NN}(E)\rangle=\frac{1}{A_1A_2}\{(Z_1Z_2+N_1N_2)\alpha_{pp}(E)+(Z_1N_2+Z_2N_1)\alpha_{pn}(E)\}. \quad (2.6b)$$

To correct for Pauli blocking we use the effective nucleon–nucleon cross section in the nuclear medium

$$\sigma_{NN}^{\text{eff}}(E)=P[E,E_{F1},E_{F2}]\sigma_{NN}^{\text{free}}(E), \quad (2.7)$$

where E_{F1} and E_{F2} are the Fermi energies of the nuclei at the point where the nucleons collide (local density approximation). The reduction factor $P[E,E_{F1},E_{F2}]$ was calculated analytically in ref. [9]). For $^{17}O+^{208}Pb$ at 84 MeV/nucleon, the averaged nucleon–nucleon cross section is reduced by a factor 0.62 as compared to the free nucleon–nucleon cross section [9]).

To avoid lengthy numerical calculations we parametrize the nuclear densities as gaussians and determine the central densities and widths by the condition that they will be a good approximation for the densities at the nuclear surfaces. This amounts to write [10])

$$\rho^{(i)}(r)=\rho_G^{(i)}\,e^{-r^2/\alpha_i^2}, \quad (2.8)$$

where $\alpha_i=\sqrt{2aR_i}$ and $\rho_G^{(i)}=\frac{1}{2}\rho_0\,e^{R_i/2a}$, with $i=1,2$; $\rho_0=0.17\ \text{fm}^{-3}$, $a=0.65$ fm and $R_i=1.2A_i^{1/3}$ fm.

Inserting (2.8) in (2.4) and expanding into multipoles to separate the projectile coordinate and the intrinsic coordinate of the target, we obtain

$$\mathcal{U}_N(\boldsymbol{r},\boldsymbol{r}')=4\pi\rho_G^{(1)}\langle t_{NN}\rangle\,e^{-r^2/\alpha_1^2}\,e^{-r'^2/\alpha_1^2}\,\rho_2(\boldsymbol{r}')\sum_{l,m}(-i)^l Y_{lm}(\hat{\boldsymbol{r}})\,Y_{lm}^*(\hat{\boldsymbol{r}}')\,j_l\left[\frac{2irr'}{\alpha_1^2}\right]. \quad (2.9)$$

As a next step we calculate $\langle\boldsymbol{r},\lambda\mu|U_N(r)|\boldsymbol{r},0\rangle$ by means of the hydrodynamical model of Bohr–Tassie [7]) for the transition density $\langle\lambda\mu|\rho_2(\boldsymbol{r}')|0\rangle$. In this model, the transition density of the target nucleus is related to the derivative of its ground-state density by [11])

$$\begin{aligned}\langle\lambda\mu|\rho_2(\boldsymbol{r}')|0\rangle&=-\frac{\beta_\lambda R_2^{2-\lambda}}{\sqrt{2\lambda+1}}\,r'^{\lambda-1}\frac{d\rho_2(\boldsymbol{r}')}{dr'}\,Y_{\lambda\mu}^*(\hat{\boldsymbol{r}}')\\&=2\frac{\rho_G^{(2)}}{\alpha_2^2}\frac{\beta_\lambda R_2^{2-\lambda}}{\sqrt{2\lambda+1}}\,r'^{\lambda}\,e^{-r'^2/\alpha_2^2}\,Y_{\lambda\mu}^*(\hat{\boldsymbol{r}}'), \quad (2.10)\end{aligned}$$

where β_λ is adjusted to reproduce the strength of the excitation.

Using (2.4)–(2.10) the matrix element $\langle\boldsymbol{r},\lambda\mu|U_N(\boldsymbol{r})|\boldsymbol{r},0\rangle$, which appears in (2.2) can be straightforwardly evaluated. After integrating over the intrinsic coordinate

of nucleus 2, using the integral

$$\int_0^\infty r^{\lambda+2} j_\lambda(pr)\, \mathrm{e}^{-q^2r^2}\, \mathrm{d}r = \sqrt{\frac{\pi}{2}}\, \frac{p^\lambda}{(2q^2)^{\lambda+3/2}}\, \mathrm{e}^{-p^2/4q^2}$$

we obtain

$$\begin{aligned}\langle \boldsymbol{r}, \lambda\mu | U_{\mathrm{N}}(\boldsymbol{r}) | \boldsymbol{r}, 0\rangle &= 4\pi \rho_{\mathrm{G}}^{(1)} \langle t_{\mathrm{NN}}\rangle\, \mathrm{e}^{-r^2/\alpha^2_1} \sum_{l,m} (-i)^l Y_{lm}(\hat{\boldsymbol{r}}) \\ &\quad \times \int \mathrm{e}^{-r'^2/\alpha_1^2} j_l\left[\frac{2irr'}{\alpha_1^2}\right] Y^*_{lm}(\boldsymbol{r}') \langle \lambda\mu | \rho_2(\boldsymbol{r}') | 0\rangle\, \mathrm{d}^3 r' \\ &= C_\lambda r^\lambda\, \mathrm{e}^{-r^2/\alpha^2}\, Y^*_{\lambda\mu}(\hat{\boldsymbol{r}})\,, \end{aligned} \tag{2.11a}$$

where $\alpha^2 = \alpha_1^2 + \alpha_2^2$ and

$$C_\lambda = 2\pi^{3/2} \langle t_{\mathrm{NN}}\rangle \rho_{\mathrm{G}}^{(1)} \rho_{\mathrm{G}}^{(2)}\, \frac{\beta_\lambda R_2^{2-\lambda}}{\sqrt{2\lambda+1}}\, \frac{\alpha^{2\lambda+3}}{\alpha_2^2 \alpha_1^{2\lambda}}\,. \tag{2.11b}$$

Inserting (2.11) in (2.2) and integrating over the azimuthal angle, the nuclear amplitude becomes

$$f_{\mathrm{N}}^{\lambda\mu}(\theta) = \frac{ki^{\mu+1}}{\hbar v}\, C_\lambda \int_0^\infty \mathrm{d}b\, b J_\mu(q_t b)\, \mathrm{e}^{i\chi(b)} \int_{-\infty}^\infty \mathrm{d}z\, r^\lambda\, \mathrm{e}^{(i\omega z/v - r^2/\alpha^2)}\, Y_{\lambda\mu}(\theta_{\hat{r}}, 0)\,, \tag{2.12}$$

where $r = \sqrt{b^2+z^2}$ and $\cos\theta_r = z/r$.

In the above expression we used $q_z = k_{\mathrm{i}} - k_{\mathrm{f}} \cos\theta \simeq \omega/v$, where $\hbar\omega$ is the energy transfer in the reaction. This approximation is well justified for small scattering angles and large relative motion energies. The transverse momentum q_{t} is equal to $2k \sin\frac{1}{2}\theta$ where θ is the scattering angle. We shall consider the giant resonance as a single level above the ground state, with $\hbar\omega$ equal to the giant resonance energy.

The nuclear phase shift $\chi_{\mathrm{N}}(b)$ which enters eq. (2.3) can be obtained in a closed form if one uses a gaussian parametrization of the densities, as given by eq. (2.8). It results in [10])

$$\chi_{\mathrm{N}}(b) = -\pi^2 \frac{k}{E} \langle t_{\mathrm{NN}}\rangle \left[\frac{\alpha_1^3 \alpha_2^3}{\alpha^2}\right] \rho_{\mathrm{G}}^{(1)} \rho_{\mathrm{G}}^{(2)}\, \mathrm{e}^{-b^2/\alpha^2}\,. \tag{2.13}$$

The Coulomb phase $\chi_{\mathrm{C}}(b)$, in the case of a gaussian distribution of charge for both nuclei, was derived by Fäldt [12]) as

$$\chi_{\mathrm{C}}(b) = \frac{2Z_1 Z_2 \alpha_0}{v/c} \left[\ln(kb) + \tfrac{1}{2} E_1[b^2/R_{\mathrm{G}}^2]\right], \tag{2.14}$$

where α_0 is the fine structure constant, and the exponential integral $E_1(x)$ is defined by

$$E_1(x) = \int_x^\infty \frac{\mathrm{e}^{-t}}{t}\, \mathrm{d}t\,. \tag{2.15}$$

The Coulomb phase $\chi_C(b)$ is finite for $b=0$, yielding

$$\chi_C(0)=\frac{2Z_1Z_2\alpha_0}{v/c}[\ln(kR_G)-C],$$

where $C=0.577\ldots$ is the Euler constant. For R_G we use α, introduced in eq. (2.11).

The first term of the Coulomb phase in eq. (2.14) is the contribution of a point-like charge distribution and agrees with the result obtained from the angular momentum expansion of the elastic Coulomb amplitude. This term is of crucial relevance to determine the appropriate dependence of the inelastic differential cross section. The second term inside the parentheses of eq. (2.14) is a correction for the consideration of a gaussian distribution of charge [12]). As we verified above, it eliminates the divergence of the Coulomb phase for a point charge distribution at $b=0$.

In the case of the Coulomb interaction the transition matrix in (2.2b) becomes

$$\langle \boldsymbol{r}, \lambda\mu|U_C(\boldsymbol{r})|\boldsymbol{r}, 0\rangle = Z_1e^2\int\langle \boldsymbol{r}, \lambda\mu|\frac{\rho_2(\boldsymbol{r}')}{|\boldsymbol{r}-\boldsymbol{r}'|}|\boldsymbol{r}, 0\rangle\,\mathrm{d}^3r'$$

$$=4\pi Z_1e^2\sum_{l,m}\frac{1}{(2l+1)}\frac{1}{r^{l+1}}Y_{lm}(\hat{\boldsymbol{r}})\mathcal{M}(\mathrm{E}l, m), \qquad (2.16)$$

where

$$\mathcal{M}(\mathrm{E}l, m)=\int r'^lY^*_{lm}(\hat{\boldsymbol{r}}')\langle\lambda\mu|\rho_2(\boldsymbol{r}')|0\rangle\,\mathrm{d}^3\boldsymbol{r}', \qquad (2.17)$$

are the electric multipole moments of nucleus 2. We only consider monopole-multipole interaction, assuming the projectile to be a point charge distribution.

Using the Bohr-Tassie model to infer $\mathcal{M}(\mathrm{E}\lambda, \mu)$ in eq. (2.2b) and performing the integral in the azimuthal angle, we obtain

$$f_C^{\lambda\mu}(\theta)=\frac{ki^{\mu+1}}{\hbar v}D_\lambda\int_0^\infty \mathrm{d}b\,bJ_\mu(q_ib)\,\mathrm{e}^{i\chi(b)}\int_{-\infty}^{\infty}\mathrm{d}z\,\mathrm{e}^{i\omega z/v}\frac{1}{r^{\lambda+1}}Y_{\lambda\mu}(\theta_{\hat{r}}, 0), \qquad (2.18a)$$

where

$$D_\lambda=\pi^{3/2}Z_1e^2\rho_G^{(2)}\frac{\beta_\lambda R_2^{2-\lambda}(2\lambda-1)!!\,\alpha_2^{2\lambda+1}}{2^{\lambda-1}\sqrt{2\lambda+1}}. \qquad (2.18b)$$

The integrals in eqs. (2.12) and (2.18) are performed numerically. The differential cross section of the excitation of a λ-pole state is given by

$$\frac{\mathrm{d}\sigma_\lambda}{\mathrm{d}\Omega}=\sum_\mu|f_N^{\lambda\mu}(\theta)+f_C^{\lambda\mu}(\theta)|^2. \qquad (2.19)$$

Due to the prescription which we used to construct the nuclear potential and excitation amplitude, we foresee that the β_λ values which appear in eq. (2.10) are not equal for the nuclear and for the Coulomb excitation amplitudes. For example,

the nuclear excitation of isovector giant dipole resonances (IVGD) are dependent on the neutron (or proton) excess of the target. If $Z_2 = N_2$ and the proton and nuclear radii are equal, the excitation of IVGD states in the target can be accomplished only if the coupling of the projectile to neutron and proton are different. This is always the case for the Coulomb interaction but not for the nuclear one, at least in the way that we postulated it. On the other hand, the excitation of isoscalar giant quadrupole states (ISGQ) can result from both Coulomb or nuclear interaction. In the applications of the next section we shall use $\beta_1^{\mathrm{N}} = 0$ and $\beta_2^{\mathrm{N}} \simeq \beta_2^{\mathrm{C}}$.

The deformation parameters $\beta_\lambda^{\mathrm{C}}$ can be related to the reduced matrix elements for electromagnetic transitions. Using sum rules for the reduced matrix elements, one finds

$$\beta_1^{\mathrm{C}} R = \sqrt{\frac{2\pi N\hbar^2}{AZmE}}, \qquad \beta_2^{\mathrm{C}} R = \sqrt{\frac{20\pi\hbar^2}{3AmE}}, \tag{2.20}$$

where R is the mean radius of the target nucleus; m is the nucleon mass and E is the excitation energy.

3. Results and discussion

We can write the integrals (2.12) and (2.18) as

$$f_{\mathrm{C,N}}^{\lambda\mu}(\theta) = ik \int_0^\infty \mathrm{d}b\, bJ_\mu(q_t b)\Gamma_{\mathrm{C,N}}^{\lambda\mu}(b), \tag{3.1}$$

where $\Gamma_{\mathrm{C,N}}^{\lambda\mu}(b)$ are interpreted as the Coulomb (nuclear) excitation strength for a given impact parameter b. They are given in terms of integrals over the variable z, exhibited in eqs. (2.12) and (2.18).

The main contribution to these integrals comes from the region around $z = 0$. If we use the approximation $Y_{\lambda\mu}(\theta_r, 0) \simeq Y_{\lambda\mu}(\frac{1}{2}\pi, 0)$, the excitation strength functions $\Gamma_{\mathrm{C,N}}^{\lambda\mu}(b)$ may be calculated analytically. The results are

$$\Gamma_{\mathrm{N}}^{\lambda\mu}(b) = \frac{\sqrt{\pi}\alpha}{\hbar v} i^\mu C_\lambda Y_{\lambda\mu}(\tfrac{1}{2}\pi, 0) b^\lambda \, \mathrm{e}^{[i\chi(b) - (\omega\alpha/2v)^2 - (b/\alpha)^2]}, \tag{3.2}$$

and

$$\Gamma_{\mathrm{C}}^{\lambda\mu}(b) = \frac{2\pi}{\hbar v} \frac{i^\mu D_\lambda}{\Gamma[\frac{1}{2}(\lambda+1)]} Y_{\lambda\mu}(\tfrac{1}{2}\pi, 0)[2b]^{-(\lambda+1)/2} \left(\frac{\omega}{v}\right)^{(\lambda-1)/2} \mathrm{e}^{[i\chi(b) - \omega b/v]}, \tag{3.3}$$

The validity of these approximations was checked numerically comparing them to the solution of eqs. (2.12) and (2.18) for $^{17}\mathrm{O} + ^{208}\mathrm{Pb}$ at 84 MeV/nucleon. The error in the differential cross sections was found to be less than 5%. Therefore, the calculation of the differential cross section for the excitation of giant resonances in intermediate-energy collisions can be reduced to the evaluation of a single integral over impact parameters.

In fig. 1 we show the differential cross section for the excitation of the isovector electric dipole resonance with energy $E_{GDR} = \hbar\omega = 13.5$ MeV in ^{208}Pb by means of ^{17}O projectiles at 84 MeV/nucleon laboratory energy. In these calculations we used $\langle\sigma_{NN}\rangle = 60$ mb and $\langle\alpha_{NN}\rangle = 1$. The experimental data, represented by black dots, are taken from ref. [1]). We see that the Coulomb amplitude alone is capable to reproduce the data quite well. Since the Coulomb interaction is known very well, this exhibits the fact that the excitation of IVGDR in heavy-ion collisions at intermediate energies is a powerful tool to investigate the properties of such states [1]). A deformation length of $\beta_1 R = 0.42$ fm was used, which corresponds to 113% of the energy weighted sum rule result given by eq. (2.20). It must be borne in mind that when we use $f_N = 0$, it does not mean that the nuclear interaction does not participate in the excitation process, since it always contributes appreciably to the phase $\chi(b)$. It causes the distortion of the elastic scattered wave which is essential for the correct calculation of the excitation amplitude (DWBA). Also, the Coulomb phase is very important since it is responsible for the broad peak of the differential cross section, just in the region where the experimental data are available. The peaks at low scattering angles and the wiggling of the cross section at large angles are caused by nuclear diffraction.

Fig. 2 shows the same differential cross section, but for the excitation of a giant quadrupole state with energy of 10.6 MeV in ^{208}Pb by means of ^{17}O projectiles at incident energy of 84 MeV/nucleon. The experimental data represented by black dots are taken from ref. [1]). A deformation length of $\beta_2 R = 0.55$ fm was used, which corresponds to 87% depletion of the energy weighted sum rule result of eq. (2.20). The short dashed line corresponds to the contribution of the nuclear amplitude,

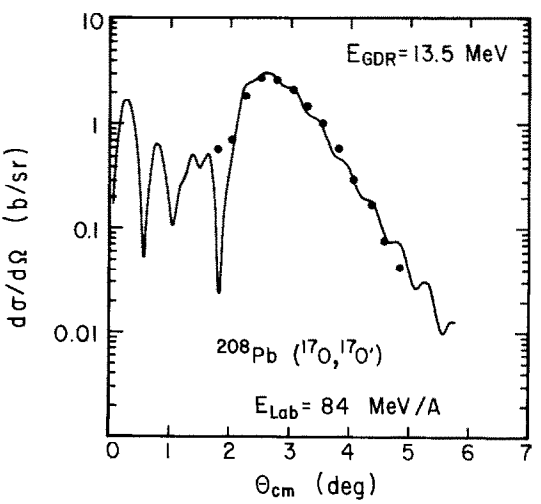

Fig. 1. Differential cross section for the excitation of isovector giant dipole resonance in ^{208}Pb by means of ^{17}O projectiles at 84 MeV/nucleon. Full dots represent the experimental data which were taken from ref. [1]). The solid line is the result of numerical calculations of eqs. (2.18) and (2.19). We used the values $\beta_1^N R_2 = 0$ and $\beta_1^C R_2 = 0.42$ fm.

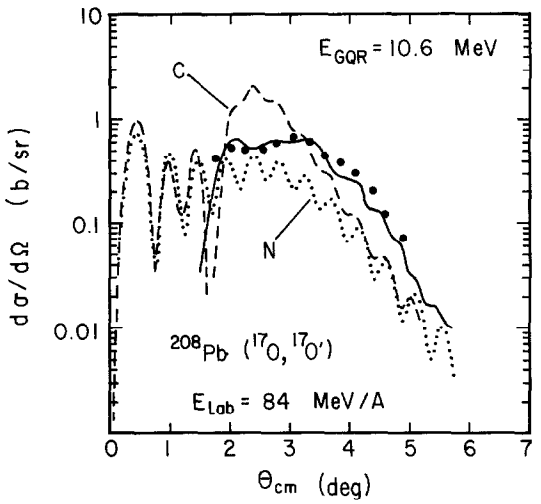

Fig. 2. Same as in fig. 1, but for the excitation of the isoscalar giant quadrupole resonance. Full dots represent the experimental data which were taken from ref. [1]). Also are shown the nuclear (dotted line), Coulomb (dashed line) and total (solid line) contributions to the differential cross section based on numerical calculations of eqs. (2.12), (2.18) and (2.19), respectively. We used the values $\beta_2^N R_2 = \beta_2^C R_2 = 0.55$ fm.

while the long dashed line corresponds to the contribution of the Coulomb interaction. The solid line results from both contributions, plus the interference between them. We observe that for the excitation of ISGQ states the nuclear contribution to the excitation is large, and may be viewed as the result of a *tidal* pull which the nuclear force acts on the target as the projectile passes by it.

The agreement between the numerical calculations and the experimental results are remarkably good, in spite of the simplicity of our approach. The deformation parameters used to fit the data are in very close agreement to the theoretical analysis of Bertrand and collaborators [1,13]), using a DWBA calculation.

The origin of the broad peaks (on a wiggly background) in figs. 1 and 2 are better understood if one compares the results of the quantum calculation as performed here with the semiclassical calculation of Coulomb excitation. Such calculations were carried out in ref. [6]), where retardation and relativistic effects on Coulomb excitation at intermediate energies were taken into account. The semiclassical calculations depend strongly on the adiabaticity parameter $\xi(\theta) = (\omega a/v)\cot\frac{1}{2}\theta$. For too small θ, $\xi(\theta) \ll 1$, and the semiclassical cross section $(d\sigma/d\Omega)_{sc}$ is negligible [6]). Only when $\xi(\theta)$ becomes appreciable as compared to unity, does the differential cross section have a large value. Therefore, as a function of θ the semiclassical cross section $(d\sigma/d\Omega)_{sc}$ increases rapidly, until it reaches an approximately constant value, just at the angular region of the broad peak from the quantum calculation. In other words, the semiclassical calculations point to the relevant angular interval of the differential cross section, where the Coulomb excitation

becomes dominant. It is clear from figs. 1 and 2 that diffraction, which is not included in the semiclassical calculations, plays a fundamental role for the correct description of the differential cross section.

The integrands in eq. (3.1) are strongly oscillating and the main contributions to the integrals comes from the b-values satisfying the stationary phase condition

$$q_t = \mathrm{Re}\left\{\frac{\mathrm{d}\chi(b)}{\mathrm{d}b}\right\}, \tag{3.4a}$$

where the right-hand side means the absolute value of the real part of the derivative of the eikonal phase with respect to b.

A semiclassical calculation of the momentum transfer in a collision with impact parameter b results in

$$q_t^{\mathrm{C}} = \frac{Z_1 Z_2 e^2}{\hbar v b}. \tag{3.4b}$$

If we interpret q_t given by eq. (3.4a) as the most probable momentum transfer for a given impact parameter and compare it to the classical value (3.4b) we obtain the result displayed in fig. 3, with the solid [dashed] line resulting from the use of eq. (3.4a) [(3.4b)]. We observe that q_t is equal to the classical value only for b greater than 15 fm. At lower impact parameters, q_t passes through a minimum around $b = 12.8$ fm, where the Coulomb repulsion and nuclear attraction equilibrate each other. Interference appears from impact parameters on different sides of this point contributing to the same value of q_t. Thus, for $q_t \lesssim 2\ \mathrm{fm}^{-1}$, corresponding to $\theta \lesssim 3.2°$, the cross section should show accentuated interference effects. Larger values of q_t

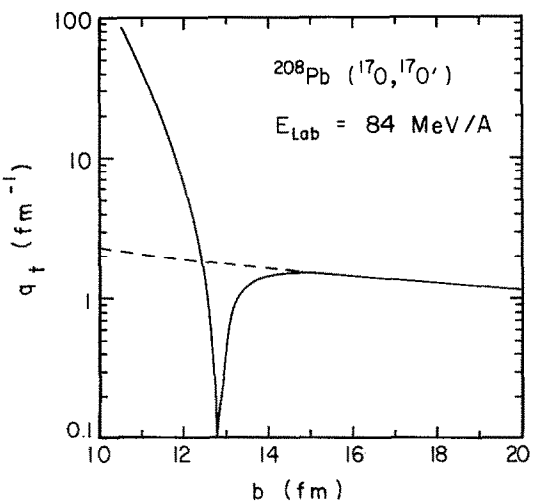

Fig. 3. Momentum transfer resulting from the stationary phase condition on the eikonal integrals as expressed by eq. (3.4a). The momentum transfer due to the Coulomb repulsion alone is exhibited by the dashed line (eq. (3.4b)).

should be suppressed by a strong attenuation manifested through the imaginary part of $\chi(b)$. These arguments explain the behaviour of the cross section, and practically all physics behind the reaction mechanism.

5. Conclusions

We have developed a simple approach to excitation of giant resonances in heavy-ion collisions at intermediate energies, based on the distorted-wave impulse approximation, eikonal wavefunctions, and the Tassie model for calculation of the transition density of the excited nucleus. In such approach, questions like the spatial origin of nuclear plus Coulomb interference, or the connection to semiclassical calculations are easily understood.

This procedure has shown that the main ingredients of the reaction mechanism are of geometrical origin and presents an advantage over the more complicated DWBA calculations, ususally referred to in the analysis of the experimental data [1,13]).

The Coulomb excitation of giant resonances with heavy-ion collisions in intermediate and relativistic energies is a rapidly growing field to obtain useful information on the nuclear structure. From the theoretical point of view there remain questions like the effects of retardation and relativistic kinematics in intermediate-energy collisions. Such effects were shown to be of relevance in ref. [6]). The Glauber approach to the inelastic process as described above provides a natural basis for the incorporation of such effects in the inelastic cross sections. Work in this direction is in progress.

We are grateful to Prof. A. Winther for useful suggestions and critical reading of the manuscript. This work was supported partially by the Conselho Nacional de Desenvolvimento Científico e Tecnológico, CNPq/Brazil.

References

1) F.E. Bertrand, J.R. Beene and D.J. Horen, Nucl. Phys. **A488** (1988) 163c
2) R.J. Glauber, Lectures on theoretical physics (Interscience, New York, 1959) vol. 1
3) R.A. Broglia, C.H. Dasso, H. Esbensen, A. Vitturi and A. Winther, Nucl. Phys. **A345** (1980) 263
4) A. Vitturi and F. Zardi, Phys. Rev. **C36** (1987) 1404;
S.M. Lenzi, A. Vitturi and F. Zardi, Phys. Rev. **C38** (1988) 2086
5) K. Alder and A. Winther, Electromagnetic excitation (North-Holland, Amsterdam, 1975)
6) A.N.F. Aleixo and C.A. Bertulani, Nucl. Phys. **A505** (1989) 448
7) L.J. Tassie, Austral. J. Phys. **9** (1956) 407
8) A.K. Kerman, H. McManus and R.M. Thaler, Ann. of Phys. **8** (1959) 551
9) C.A. Bertulani, Rev. Bras. Fis. **16** (1986) 380
10) P.J. Karol, Phys. Rev. **C11** (1975) 1203
11) G.R. Satchler, Nucl. Phys. **A472** (1987) 215
12) G. Fäldt, Phys. Rev. **D2** (1970) 846
13) J.R. Beene *et al.*, Phys. Rev. **C41** (1990) 920